NLUAstro 2, 29-41 (2020) Notices of Lancaster University Astrophysics PHYS369: Astrophysics Group project

On the Origin of Hyper-Velocity Stars Near Sagittarius A**

George Greenyer[1], Antonio Coulton[1], Josh Smith[1], Rhys Jaques [1], Nathan Wright[1], Keenan Wright[1] & David Sobral[1]†
[1] *Department of Physics, Lancaster University, Lancaster, LA1 4YB, UK*

Accepted 19 June 2020. Received 31 May 2020; in original form 20 March 2020

ABSTRACT

We present our investigation into the origins of high- and hyper-velocity stars around the Milky Way by exploring *Gaia* data. We begin by establishing a working set of criteria for a star to even be considered as a potential hyper-velocity star, which we defined chronologically as: if the uncertainty in parallax is acceptably low; if the star has above average total velocity for its home set; and finally if the star has mostly radial velocity, we will investigate it further. We also discuss the complications encountered trying to identify candidate stars. Finally, we perform a time-reversing procedure to trace our final set of stars back to where they may have originated. We found a large number of candidate stars in our initial broad range search, but by enforcing stricter constraints we found a final sample of 1,158 potential hyper-velocity stars. This set displayed zero stars passing close enough to Sagittarius A* to have been thrown out or boosted to their current velocities. However, by selecting hyper-velocity stars with little proper motion in right ascension and declination, we discovered five stars which may have passed close enough to Sagittarius A* to have had their orbits significantly altered. A detailed analysis of the trajectories of those stars was performed, resulting in one star that may have originated from a binary system that had a close encounter with Sagittarius A*. We propose a potential binary partner in some of the known stars orbiting Sagittarius A* with similar periapsis.

Key words: High Velocity Stars, Hyper-velocity Stars, Hills Mechanism, Slow Intruder, Python, Gaia, Sagittarius A*.

1 INTRODUCTION

In the early 1960s Adriaan Blaauw (Blaauw 1961) postulated a hypothesis to explain the high space velocities of several observed stars; he named these *Runaway Stars*. These first observed runaway stars, ranging from type O5 to type B5, were travelling at considerable velocities, with some nearing 200kms^{-1}, as opposed to the more common velocities of below 30 km s^{-1}.

In order to explain the velocities of runaway stars Blaauw proposed what is now commonly known as the *Supernova Kick Mechanism* (Brown 2015; Erkal et al. 2019; Hattori et al. 2019; Hoogerwerf et al. 2001). This mechanism attributes the high space velocities of runaway stars to one star in a binary star system undergoing a supernova explosion. When the more massive, shorter lifetime star explodes it results in the less massive companion star being repelled at considerable velocity. What happens next is dependent upon the direction of the runaway star's velocity. If it is aligned with the rotation of the Galaxy then, depending upon the distance of the star from the galactic centre (GC), it may become unbound from the Galaxy. If the direction of velocity of the star is opposed to the rotation of the Galaxy then it is more likely that the star will remain galactically bound as its effective velocity will be smaller due to its galactic rotation velocity opposing its ejection velocity (See also Leonard & Duncan 1990; Hoogerwerf et al. 2001; Irrgang et al. 2019).

A few years later, after analysing the motion of other runaway stars, Poveda et al. (1967) proposed an additional mechanism explaining the velocities of runaway stars which could not be explained by the supernova kick mechanism. The motion of these stars was observed to not originate from a supernova, but rather from a collapsed proto-stellar galactic cluster. Poveda et al. theorised that the process of collapse of these clusters resulted in dynamical interactions (Chatterjee & Tan 2012, for example) that could result in high velocities for stars escaping the cluster. Throughout the

* Based on observations obtained with ESA's *Gaia* space observatory.
† PHYS369 supervisor

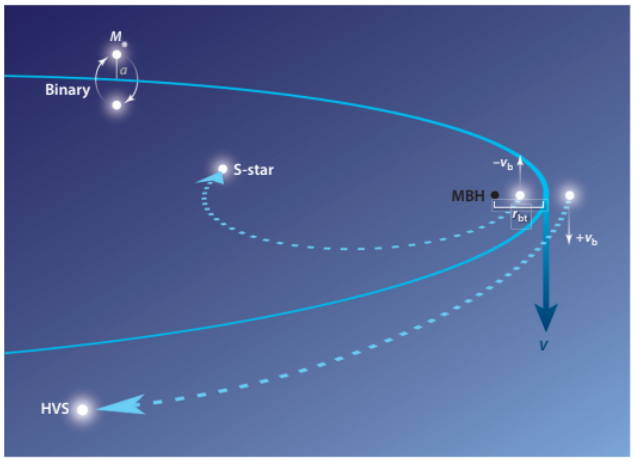

Figure 1. Diagram depicting the Hills mechanism. It can be seen that the black hole captures the closer star, resulting in the ejection of the farther star at high velocity. Figure inspired by J. Guillochon (Brown 2015)

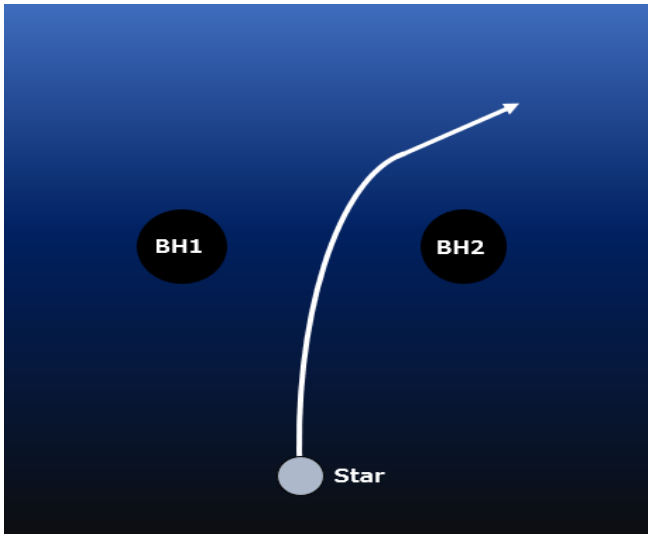

Figure 2. Diagram depicting the Slow Intruder Scenario. The black holes have unequal mass, in this case $M_{blackhole2} > M_{blackhole1}$. As the star passes between the black hole binary it experiences greater gravitational force towards the more massive black hole and its trajectory is altered accordingly. This results in the star being ejected from the system as a high-velocity star.

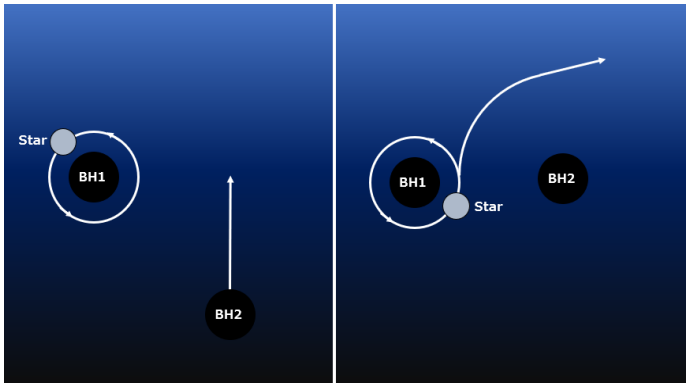

Figure 3. Diagram depicting the Bound Scenario. In the case in which a star is orbiting a black hole, another black hole may approach this system, causing the orbit of the star to be destabilised and thus resulting in the star being ejected as a high velocity star.

rest of the paper we shall refer to this as the *Poveda Mechanism* (See also Hattori et al. 2019; Capuzzo-Dolcetta & Fragione 2015). These runaway stars can also subsequently undergo a slingshot interaction with a black hole, accelerating the runaway star to the extent that it becomes a *hyper-velocity star*.

In 1988, Hills (1988) analysed the motion of hyper-velocity stars whose origins could not be explained by either of the aforementioned mechanisms, and proposed the *Hills Mechanism*. This mechanism involves an interaction in which a massive black hole (MBH) captures a star from a binary pair, resulting in the other star being ejected from the binary with very high velocity (see Fig.1). The Hills mechanism has been attributed as the originator of high velocity stars with speeds exceeding 1000kms^{-1}. There does not necessarily exist an exact, uniform definition of hyper-velocity stars, and definitions can vary between papers as per their specific objectives; our definition is provided in our *methodology* section.

More recently, Yu & Tremaine (2003) published a paper suggesting a new mechanism capable of producing hyper-velocity stars involving a binary black hole (BBH) interacting with a single star. Commonly referred to as the *Slow Intruder Scenario* (Darbha et al. 2019), this case describes a star being attracted towards the more massive black hole as it passes in between the BBH and gaining a velocity boost. The star is subsequently ejected as a hyper-velocity star (see Fig.2). This three body system of two black holes and a single star can also produce HVS' in the *Bound Scenario*, in which a MBH being orbited by a star is approached by a second black hole disrupting the orbit and causing the star to be ejected with high velocity (see Fig. 3, Gualandris et al. 2005 and Darbha et al. 2019). These scenarios are still possible within the Milky Way as a BBH in the Galactic centre has not yet been ruled out (e.g. Rasskazov et al. 2019; Yu & Tremaine 2003; Herrnstein et al. 2004).

One final mechanism to be considered is when a dwarf galaxy makes a *pericentric passage*, pericentric meaning the point in an orbit nearest the centre of gravity of which the body orbits, of the larger galaxy (Abadi et al. 2009). In this scenario, the dwarf galaxy passes close to the larger one and causes a disruption of the tidal forces in the dwarf creating a stream, otherwise known as the *tidal tail*, of stars in the halo of the larger galaxy in a high-velocity orbit, occasionally exceeding the local escape velocity of the galaxy (see also Abadi et al. 2006).

Not much is currently known about hyper-velocity stars; data has been limited in previous surveys, however recently *Gaia* changed this by providing a huge number of sources with data on parameters including radial velocity and effective temperature. This paper will be able to explore the origins of this rare phenomenon with a focus on stars that likely had an origin close to Sagittarius A*. Section 2 will explain where our data came from. Section 3 will explain how the data was refined, and how the simulation was con-

structed. The results are covered in section 4, with the results being discussed and concluded in section 5, and section 6 respectively.

2 CATALOGUE

We have used data from the second data release (DR2) of ESA's *Gaia* mission to produce this study. The *Gaia* mission was originally proposed in 1993 for the ESA's Horizon+ programme with the aim of measuring the position, parallax and proper motion of at least 1 billion stars with a magnitude of 20 or brighter; this accounts for approximately 1% of the total population of the Milky Way (Liu et al. 2012). The *Gaia* satellite was successfully launched in December of 2013 with an initial mission duration of 5 years. However, at the time of writing, the *Gaia* satellite is expected to remain operational until at least 2024.

The *Gaia* satellite is equipped with three main instruments of measurement. These are composed of:

- An astrometry instrument, which, by taking repeated measurements of the same targets over the duration of *Gaia*'s mission allows for the calculation of the targets' positions, distances and proper motions (Liu et al. 2012).
- Blue and red photometers, together able to detect light between 330nm and 1050nm from stars of magnitude 20 or brighter. The data attained by these photometers can then be used to calculate the age, temperature, mass and composition of the target bodies (Jordan 2008).
- A radial-velocity spectrometer, able to calculate the velocity of stars moving either towards or away from *Gaia* by measuring the Doppler shift in the observed wavelengths (Jordan 2008).

In order to use the *Gaia* data, we applied various restrictions and produced a catalogue of 3 million stars. We then implemented some different methods to identify and study a set which we consider likely to be high velocity stars. We discuss the reasoning and methodology behind these restrictions in sections 3.1 and 3.2.

3 METHODOLOGY

3.1 Gathering our Data

Our initial sample was obtained by taking a section of the sky from the *Gaia* survey around Sagittarius A* and immediately constraining the radial velocity to greater than 500kms^{-1}. The value of 500kms^{-1} was chosen after collecting data for 3 million stars (see section 2) and looking at the Gaussian distribution for their velocities as shown in in Fig 4.

A cut off velocity of 500kms^{-1} was decided as, after reviewing Fig 4, this velocity is greater than 10σ from the mean suggesting that stars greater than 500kms^{-1} are sufficiently fast enough to fit with the usage in other papers ((Brown 2015; Marchetti et al. 2018; Boubert et al. 2019)) and faster than established high velocity stars ((Blaauw 1961; Poveda et al. 1967)).

The initial search gave us 12 candidate stars, however to avoid any bias we revised our parameters to produce a full-sky data set, which we then cut down by applying a constraint on total velocity for the body, one on parallax and one on parallax error as detailed in section 3.2. This yielded 1158 viable stars. The results from these stars are discussed in section 4.1.

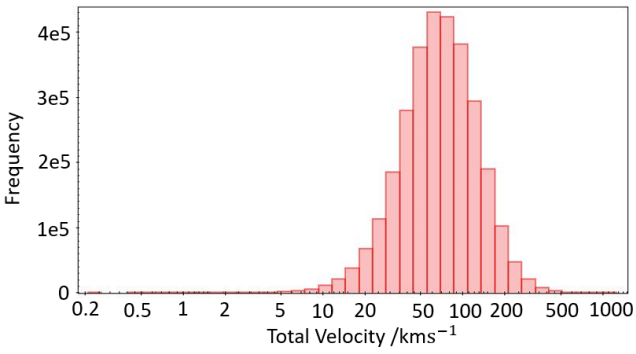

Figure 4. Gaussian distribution of total velocity of all 3 million stars in our data search.

3.2 Data Selection and Constraints

As discussed in section 2, we applied various restrictions and constraints to our sample. We originally restricted the stars in our data set to those with parallax angles between 0.001 and 1 milliarcsecond (1kpc to 1Mpc) with fractional errors in their parallax angles of 20% or less. We also only used stars which had non-zero proper motion and angular velocity.

We took our collection of 3 million stars and narrowed it down to 1158. This was done by taking all stars that fit the criteria of having a velocity of at least 500kms^{-1} as defined in section 3.1. The values of right ascension, and declination were used to converted to Cartesian velocity coordinates with:

$$v_x = -\frac{A\nu_\alpha sin(\alpha)}{\theta} - \frac{A\nu_\delta sin(\delta)cos(\alpha)}{\theta} + v_r cos(\delta)cos(\alpha) \quad (1)$$

$$v_y = \frac{A\nu_\alpha cos(\alpha)}{\theta} - \frac{A\nu_\delta sin(\alpha)sin(\delta)}{\theta} + v_r cos(\delta)sin(\alpha) \quad (2)$$

$$v_z = \frac{A\nu_\delta cos(\delta)}{\theta} + v_r sin(\delta) \quad (3)$$

where v is velocity in x, y, and z directions; A is a conversion constant equal to 4.7404; ν is the proper motion motion in right ascension (α), and declination (δ); v_r is the radial velocity; and θ is the parallax angle.

These stars were then plotted to show their position in the sky as shown in Fig 5. This plot allowed us to better select stars to find those most likely to have originated from a black hole, which could then be used in the simulation (see section 3.3).

We attempted to narrow the search to just HVS' with very small proper motion (here defined as < 1" in both right ascension and declination), see appendix A1, which returned a single star with $v = 450$kms^{-1}. Having small proper motion means that it is most likely moving directly

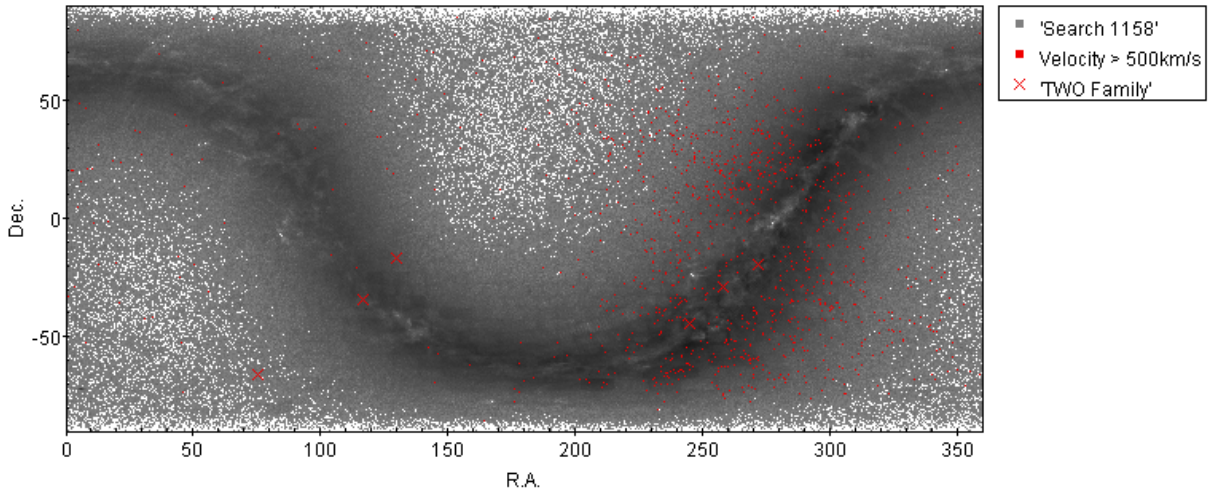

Figure 5. Position plot of all stars in the search that qualify as HVS', showing a greater concentration in the area of sky around Sagittarius A*

towards Earth and almost certainly has its origin near Sag A*. This star was named 'That Weird One' (TWO) due to the unexpected nature of its movements when simulated (see section 4). Upon allowing for a larger parallax error, this same search returned a further 4 stars, dubbed TWO-410, TWO-558, TWO-570, and TWO-599, named due to their similarity to TWO and followed by the first three digits of their *Gaia* data source ID to differentiate between them, see appendix C. Collectively, these stars have been named 'The TWO Family'.

3.3 Constructing the Simulation

3.3.1 The Original N-body Simulation

In order to predict the paths of the stars that were studied, it was necessary to construct an N-body simulation. To do this we utilised a simplified simulation built in software:PYTHON, which was based on previous work. This simulation employs a simple method of calculating the acceleration for each body in the system, along with a time-step system to update the velocities and positions of the bodies via the Euler-Cromer method. The simulation takes a list of objects to simulate. These objects are in the form of a Particle class, which contains information about the body such as:

- Name
- Position
- Velocity
- Acceleration
- Mass
- Radius

In this class, there are also functions by which the particle can update these parameters.

The list of objects was created in software:PYTHON by reading a comma-separated variable (CSV) file which contained data on the stars that were of interest to the project. This was generated using the software: TOPCAT with data from the *Gaia* survey, as discussed in section 3.1.

Once the list of bodies to simulate is defined, for each time-step the simulation iterates through a list of bodies, calculating the acceleration on each by finding the sum of the individual acceleration values on a first body due to each other body:

$$a = \sum_{i=1}^{n} \frac{Gm_i}{r_i^2} \hat{\mathbf{r}}_i \tag{4}$$

where G is the gravitational constant ($6.67408 \times 10^{11} \mathrm{m^3 kg^{-1} s^{-2}}$), m_i is the mass of the other body, r_i is the magnitude of the distance between the bodies, and $\hat{\mathbf{r}}_i$ is the unit vector of the distance between the bodies. This may be derived from a more general equation for calculating the force on a body in an N-body simulation (Trenti & Hut 2008), which in the case of no external potential may be written as follows:

$$F = -\sum_{j \neq i} \frac{Gm_i m_j (\vec{r_i} - \vec{r_j})}{|\vec{r_i} - \vec{r_j}|^3} \hat{\mathbf{r}}_i \tag{5}$$

Once this has been calculated, the Euler-Cromer method (Saroja & Nuriyah 2019) for calculating the updated velocity and distance of each body is applied:

$$v_n = v_{n-1} + a\delta t \tag{6}$$

$$x_n = x_{n-1} + v\delta t \tag{7}$$

where a is the acceleration calculated using Equation 5, v_n is the velocity for the nth time-step, x_n is the position for the nth time-step, and δt is the value of the time-step.

During each step, data is saved regarding the positions of the bodies in the system. Once a predetermined amount of time has been simulated, the simulation stops and plots a graph of the positions of the bodies of the system during the simulation. This allows for the visualisation of orbits and trajectories of bodies in the system.

In addition, there is a collision system modelled in to

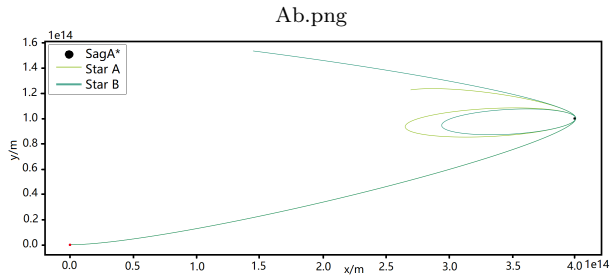

Figure 6. Test run demonstrating the paths of stars undergoing the Hills mechanism using a dummy binary system.

the simulation in which two bodies can collide and the mass of the smaller body will be added to the larger body. The momentum of the larger body will be altered by the collision. This collision model is limited in that it calculates collision on a time-step basis. If an object has a large enough velocity, it can begin the time-step on one side of an object and end it on the other side, essentially skipping over the object and not detecting a collision where one should realistically occur.

3.3.2 Subsequent Additions and Improvements

In an attempt to improve the accuracy of the simulation, an alternate version of the simulation was created which replaced the Euler-Cromer method of updating particles with a fourth-order Runge-Kutta method. This method is able to better estimate the acceleration on each particle, as it calculates the acceleration on the particle at differing points over the course of one time-step, using different initial acceleration values, then weighing the individual results and combining them to provide a final acceleration value.

3.3.3 Testing the Simulation

To ensure that the simulation performs as expected, several test simulations were ran modelling the Hills mechanism (Fig 6), the slow intruder scenario (Fig 7), and the bound scenario (Fig 8; orbital data for the star from Gillessen et al. (2017)). Sagittarius A* was used in all three of the test plots, with data for the BBH adjusted to fit with Sagittarius A* from Rodriguez et al. (2006), the mass of the intermediate mass black hole (IMBH) was taken to be $5M_\odot$ (Greene et al. 2019).

3.4 Galactic Models and Comparisons

In addition to the main simulation used for tracing the paths of the candidate stars, we also constructed a simple model galaxy in Python expressly to predict the escape velocity of objects at any distance from the galactic centre, within an approximate radius of the dark matter halo. This model is based on some found in literature (Schmidt 1956; Innanen 1971; Flynn et al. 1996), but heavily simplified in order to be completed in our time frame. We used a sum of different potentials characteristic to the different parts of the galaxy to calculate the escape velocity as:

$$v_{esc} = \sqrt{2|\Phi(r)|} \tag{8}$$

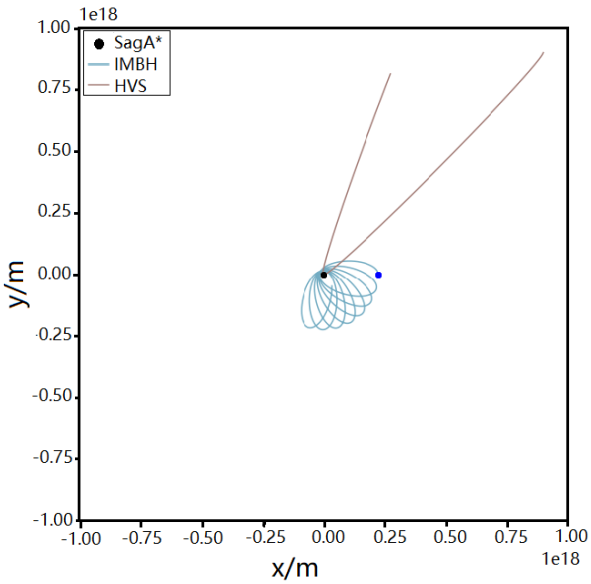

Figure 7. Test run demonstrating the paths of the star and black holes in the slow intruder scenario.

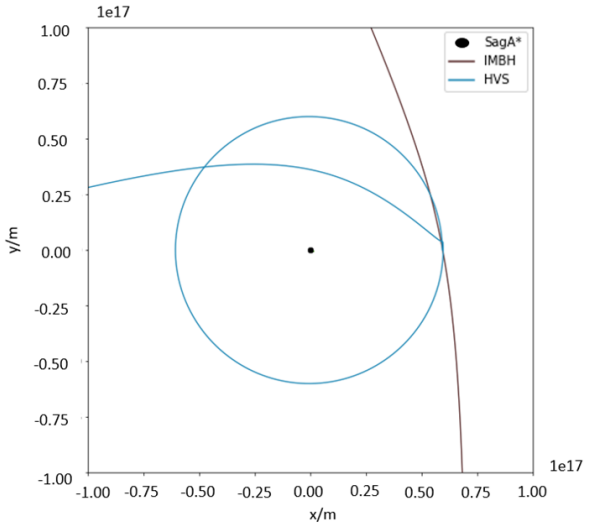

Figure 8. Test run demonstrating the paths of the star and black holes in the bound scenario.

Where $\Phi(r)$ is the total radius dependent potential.
In order to calculate this potential, we divided the galaxy into three principle components: the bulge, the disk and the dark matter halo, each with its own specifically formulated potential Φ_B, Φ_D and Φ_H respectively.
The halo potential was modelled as an individual potential as shown in equation 9, however the disk and bulge potentials were divided again into three and two sub-potentials respectively of different mass sections to more accurately model the overall mass distribution in our galaxy. This gave us the following potential behaviours:

$$\Phi_B = -\frac{GM_1}{\sqrt{r^2 + r_1^2}} - \frac{GM_2}{\sqrt{r^2 + r_2^2}} \tag{9}$$

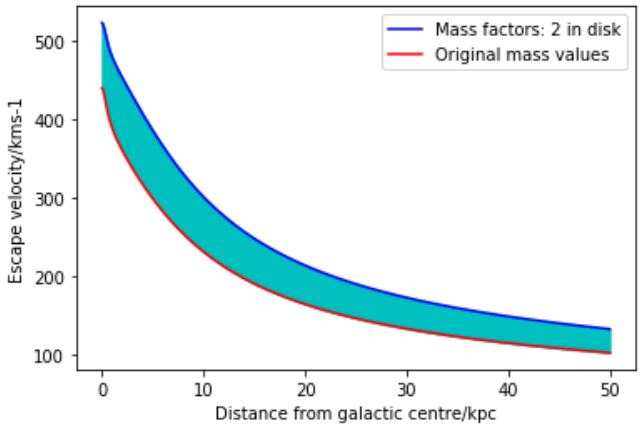

Figure 9. Escape velocity vs distance from galactic centre for a galaxy with Milky Way-like mass values and a galaxy with a disk that is twice as heavy.

for the bulge, which is recognisably close to the standard spherical potential of a point mass, implemented using two estimates of the mass of the central section of the Milky Way, contained within the radii r_1 and r_2:

$$\Phi_D = \Phi_{D1} + \Phi_{D2} + \Phi_{D3} \tag{10}$$

for the disk, where each of the sub-potentials take the form:

$$\sum_{i=1}^{3} \frac{-GM_i}{\sqrt{r^2 + (a_i + \sqrt{b^2 + z^2})^2}} \tag{11}$$

Here b is the scale thickness of the disk, chosen as a constant average value appropriate for a thick disk galaxy like the Milky Way, z is a parameter to modify the height above the galactic plane being considered, and a_i is related to the scale length of that section of disk. This potential is based on a cylindrical consideration of the galaxy, with z as the cylindrical height. Originally the dark matter halo was expected to be modelled, with a radius overlapping that incorporated by the disk potential out to an estimate of the outer edge of the galaxy, however this idea was discarded as it was unfeasible.
Equations 9 and 10 were implemented as functions in software:PYTHON which contributed to an overall summation of potential. This "toy" galaxy was then initiated twice with two separate sets of of approximate mass values (tabulated in appendix B) to produce a plot displaying an area of viable velocities at each radial distance.

All of the original values shown in table B1 except for the scale thickness value b were taken from Flynn et al. (1996). To check their validity, the code was run with various combinations of a range of values close to these. The final pair of simplified galaxies produced the graph in Fig 9.

3.5 Dynamic Mass Modelling

In order to model the mass which is having a non-negligible gravitational effect on our simulation we performed the following calculations.

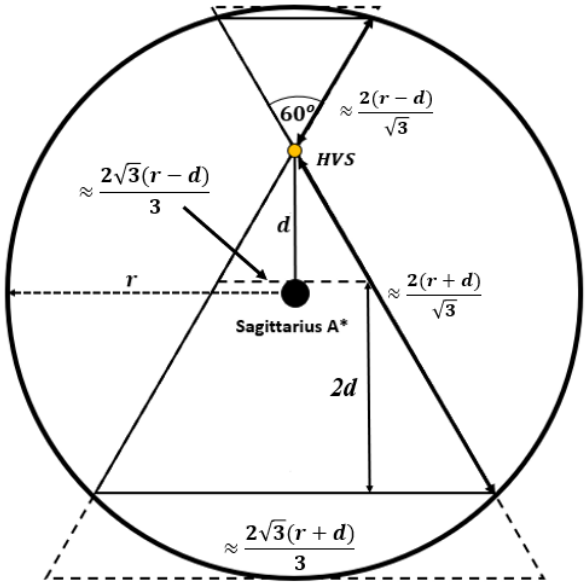

Figure 10. Diagram used to approximate the net gravitational force exerted upon a subject high velocity star due to dark matter.

3.5.1 *Luminous Matter*

In order to calculate the gravitational attraction due to luminous matter we modelled the distribution of matter with respect to distance from the galactic centre as $\frac{1}{r^2}$. We were therefore able to calculate the mass contained within a given radius with the equation:

$$M_L = \pi\xi \ln\left(\frac{d}{r_s}\right) + M_{SagA^*} \tag{12}$$

Where ξ is a constant equal to $1.368 \times 10^8 M_\odot$, M_{SagA^*} is the mass of Sagittarius A^*, taken to be $3.6 \times 10^6 M_\odot$ (Schödel et al. 2009), d is the distance of the simulated high velocity star from the galactic centre and M_L is the total luminous mass contained within the area bound by d.

3.5.2 *Dark Matter*

We also wanted to calculate the net gravitational effect of dark matter throughout the Galaxy on our subject star. In order to do this we approximated the Galaxy as a 2-dimensional circular plane. It is obvious that net gravitational force can only exist parallel to the line defined between Sagittarius A* and a given HVS, the net gravitational force perpendicular to this will always be 0 as dark matter is distributed approximately evenly throughout the Galaxy. We used various geometric arguments to reduce the region of dark matter considered to be exerting a net gravitational force upon the HVS to the trapezium bounded by dashed lines. We then multiplied by the mass of dark matter per unit area to calculate the mass and, by extension, the contribution to the gravitational field strength of dark matter.

$$g_{dm} = \frac{8\pi G \rho_{dm} dr_{gal}}{9\left(r_{gal} + d - \frac{6r_{gal}+2d^2}{3r_{gal}}\right)^2} \tag{13}$$

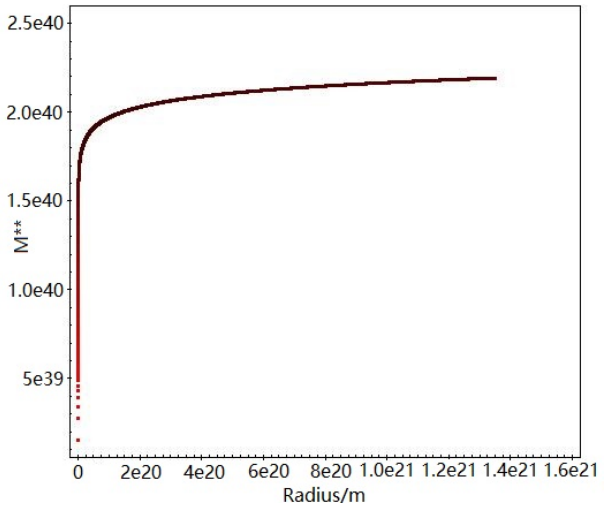

Figure 11. The effective mass of Sagittarius A* as a function of radius, with distance from Sagittarius A* on the x-axis, and the effective mass on the y-axis, as given by equation 14.

Here, G is the gravitational constant, ρ_{dm} is the mass per unit area of dark matter in the milky way, found to be 2.91kgm^{-2}. The value r_{gal} is the radius of the milky way and d is the distance between a given HVS and Sagittarius A*.

We were therefore able to model the net gravitational force acting on the HVS as acting from a single point mass located at the centre of the Galaxy with mass $M*$ as:

$$M^* = M_L + \frac{g_{dm} d^2}{G} \tag{14}$$

As such, the effective mass of Sagittarius A* changes with radius as in Fig 11, rapidly increasing before reaching a plateau, as is to be expected based on real-world observations.

3.6 Error Propagation

The initial data set that we have used from *Gaia* included errors in their measurements. These errors include uncertainties related to relativistic corrections, aberration corrections and estimation of errors in the sky background and certain assumptions about stars, amongst others. Due to the nature of these errors, they are relatively large, with the fractional errors in velocity being as large as 0.28 (28%).
To calculate the errors in both the position and velocity of our stars, we have used a Monte Carlo approach. This method works by selecting a random value that is within the margin of error for each parameter used to calculate a component of the velocity or position, and repeating this process for 150 iterations. Plotting these values results in a Gaussian distribution, and the error is then given as the standard deviation of this curve.

3.7 Mass, Lifetime and Range

Assuming the star in question is in its main sequence, its estimated lifetime can be determined by the following relation:

$$\tau = \tau_\odot \left(\frac{T}{T_\odot}\right)^{-4} \tag{15}$$

From this, should a star be on escape from the Milky Way, we can set a limit on how far the star is expected to travel during its main sequence. We can also use this to verify if it has had sufficient time to travel to its current position from Sagittarius A*. Of course, if it has not then this suggests erroneous data, or invalid assumptions made.

Similarly, the mass of the star can be estimated from a mass-temperature relation below:

$$M = M_\odot \left(\frac{T}{T_\odot}\right)^{\frac{8}{5}} \tag{16}$$

Here it is assumed the star is main sequence. Using the colour, apparent magnitude, and positional data from *Gaia*, a visual comparison on a HR diagram can verify this.

4 RESULTS

4.1 Results from Original Search ('Search 1158')

Our first set of queries resulted in 1158 stars with total velocity $v > 500$kms^{-1}, which we then sub-divided into a section of stars with total velocity $v > 700$kms^{-1} in order to ascertain a velocity distribution for the set.

When these stars were imported into the simulation and individually tested in a 2-body system with Sagittarius A*, it was observed that none of the stars (when simulated backwards in time) displayed paths consistent with a significant interaction with the black hole.

Some of the paths of the stars showed that they had indeed been affected by the gravitational pull of the black hole, but none of these apparent perturbations were significant enough to warrant a closer analysis. The paths did not deviate far from a straight line past the black hole, and many did not come close enough to the black hole for there to have possibly been an interaction such as the Hills mechanism.

4.2 Results of little proper motion stars ('The TWO Family')

The next set of queries we used loosened the constraint on radial velocity, but imposed a new set of constraints for proper motion in right ascension and declination to demand that the stars are travelling close to a line directly between Sagittarius A* and Earth. This gave us five stars with low R.A. and Dec. proper motion. From the results of passing these stars through the simulation with a variety of time steps and running times, we were able to utilise the escape velocity graph produced (see Fig. 9) to compare the stars' total velocity with the velocity with which we would expect them to be able to escape the Galaxy, and whether the simulation predicts them leaving the Milky Way if their path is uninterrupted. This "dummy check" allows us to quickly

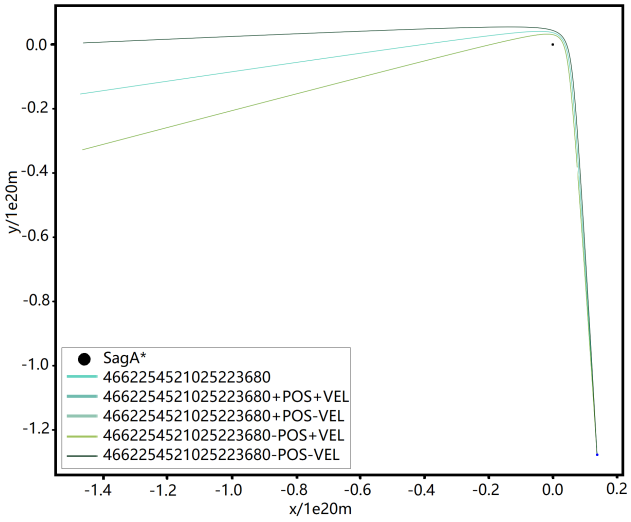

Figure 12. The trajectory of TWO in the previous 11 Myr. TWO is seen to approach Sagittarius A* from the lower right and has its orbit significantly affected by the black hole, suggesting an interaction has occurred.

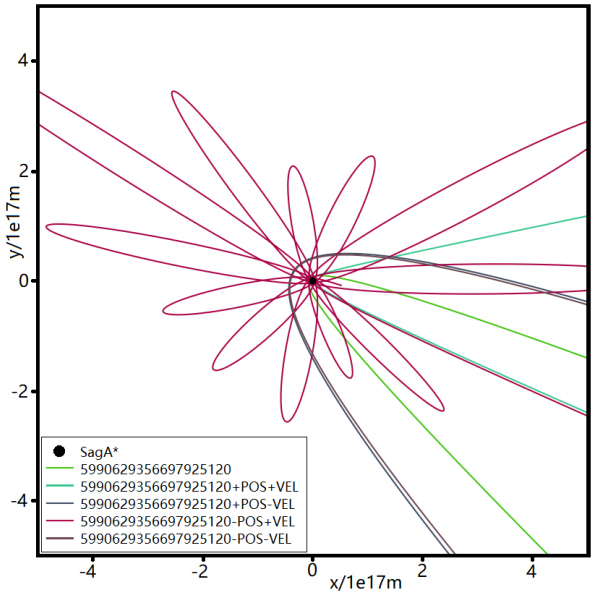

Figure 13. The trajectory of TWO-599 in the previous 1.6 Myr, focusing on the area within 5×10^{17} meters of Sagittarius A*.

identify if the results are obviously erroneous or potentially invalid.

4.2.1 TWO

TWO was the first result from the little proper motion search. While it seems that TWO had interaction with Sagittarius A* in the past 11 Myr, the star's closest approach to the galactic center was $(5.0 \pm 0.1) \times 10^{18}$m, certainly not close enough to have undergone the Hills mechanism. Other factors for its unusual trajectory, shown in Fig 12, may be in effect and we cannot rule out the possibility of TWO originating from the bound scenario or supernova kick. As discussed by Rasskazov et al. (2019), there is the possibility of an IMBH near the galactic center.

Certain properties supporting TWO's supernova kick are its mass and spectral type. Assuming TWO is main sequence, and given its temperature $T = 4695^{+111}_{-97}$K from the *Gaia* data, its mass is estimated to be $0.7^{+0.7}_{-0.6}$M$_\odot$, calculated using equation 16. This would make the star an M, K, or G class star, typical of that from a supernova kick. To more concretely confirm the star's supernova kick origin we would need to look at TWO's stellar composition, however as discussed in section 5 this was considered beyond the scope of this project.

4.2.2 TWO-410,558,570

The past trajectories of these stars are extremely similar, and are shown in appendix C, figures C1 through C3. None of these stars pass close enough to Sagittarius A* to be considered as likely having an origin at the galactic center, certainly not as close as TWO or TWO-599. While it seems TWO-558 may have approached Sagittarius A* within the errors, we still consider this error too large to make any firm conclusions from the results and so these stars must have either total velocities different to those we have determined, which is possible due to the large errors discussed in section 3.2, or originate somewhere else.

4.2.3 TWO-599

Of the TWO Family of stars, the results from TWO-599 are by far the most interesting. On a plot of TWO-599's past trajectory, Fig 13, it can be seen that the star passed very close to Sagittarius A* within the past 1.6 Myrs. Its trajectory follows close to Sagittarius A*, with various possible paths accounting for all extremes of error. One such path causes the star to be captured by Sagittarius A*, one takes it on a direct collision course with Sag A* (which obviously cannot be case as that would imply the star originated inside the black hole) and has a random trajectory from here due to limitations in the simulation. Three other paths take TWO-599 on an ordinary trajectory around Sag A*.

A plot of distance against time was produced, as shown in Fig. 14. Here we look at the distances around time -5×10^{13} seconds. It is seen that there are two potential trajectories that show a slingshot interaction, with TWO-599 approaching the black hole only once, while another is captured and approaches the black hole with some periodicity. TWO-599 has a mean closest approach of $(4.5 \pm 4) \times 10^{15}$ meters (30080 ± 13369AU). Indeed, if this were the case, then it has a similar periapsis to stars R44 and S87 Gillessen et al. (2017) at 23287^{+3346}_{-2814}AU and 17391^{+375}_{-445}AU, respectively. As such, assuming interaction through the Hills Mechanism, this would mean that it is highly likely that one of R44 or S87 may well be TWO-599's binary partner prior to interaction with Sagittarius A*. In this case, TWO-599 became the high velocity star, and R44 or S87 would be the captured partner. However, with the tools we have access to, we are unable to verify this.

Furthermore, some properties of the system can be determined should R44 or S87 be the binary partner. While we

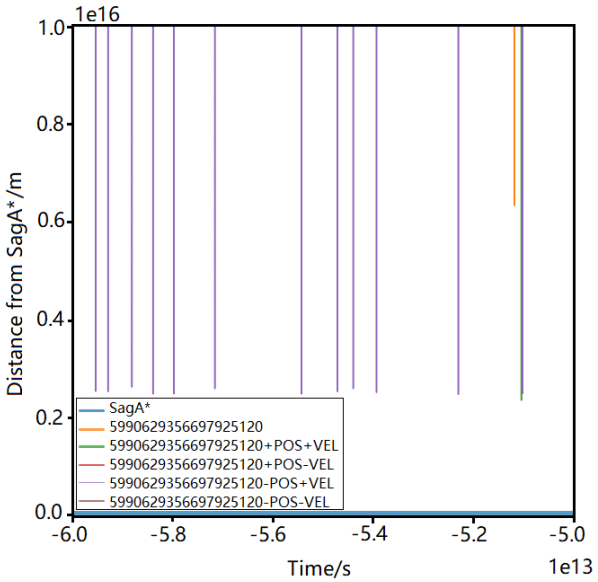

Figure 14. Magnitude of distance between TWO-599 and Sag A* around time -5×10^{13} seconds, showing multiple approaches.

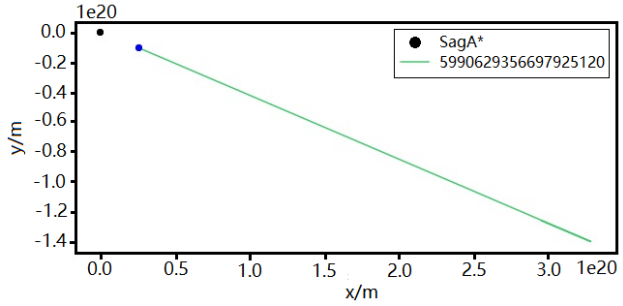

Figure 15. The expected trajectory of TWO-599 in the next 80 Myr. The Galactic Center is at the coordinate origin, and the current position of TWO-599 is indicated with a bold spot.

know TWO-599 has a mass $0.49 M_\odot$ (assuming it follows the mass-temperature relation as given in equation 16), the mass of R44 or S87 can only be estimated. Based on data provided in Habibi et al. (2017) and taking apparent magnitudes and known masses for select stars near the galactic center, we can estimate the mass of R44 and S87. Star S2 has an apparent magnitude of 14.1 in the K-band and a mass $13.6^{+2.2}_{-1.8} M_\odot$. Similarly, we can take the K-band apparent magnitudes of R44 and S87 from Gillessen et al. (2017) as 14. and 13.6 respectively, and make the approximation that they are of a similar distance, if not closer to Earth. This would mean that they would have similar luminosities, and therefore mass. Hence, we can set an upper limit on the masses of R44 and S87 as $13.6 M_\odot$.

TWO-599's future trajectory was also investigated. As per Fig. 9, and given TWO-599's current velocity of 400 ± 6 kms^{-1} and its current distance from the galactic center 891.7 ± 0.3pc, the star is not expected to escape from the Milky Way Galaxy, as seen in Fig. 15.

5 DISCUSSION

5.1 Assumptions

Our model assumes a static Galaxy in which only the star we are investigating moves, which is valid for relatively short periods of time but fails over a large time scale such as a stellar lifetime. Therefore we can run our simulation backwards or forwards to see where a star may have originated or where it may be heading if its orbit remains unperturbed, but this hypothetical path becomes less valid as the time scale increases, and also loses validity as it heads to regions of the Galaxy with a high density of bodies such as close to Sagittarius A*. Given the low number of bodies in each run of the simulation, we incorporated the mass of all luminous matter, and dark matter on the far side of Sagittarius A* to better represent the gravitational effects on the hyper-velocity star. We assumed that all of this additional mass could be added to the mass of Sagittarius A* as detailed in section 3.5.2. The result of adding this was small, but not negligible. One final assumption that we made is that Newtonian mechanics are valid in all parts of the simulation. While we would have preferred to incorporate relativity, the computational power required, as well as the time to fully code it was beyond the time frame of the project.

5.2 Simulation

Creating a non-stationary galaxy simulation would be a massive step up in required hours, research and computational power, so this is a hard limit on the scope of our project, however the short range results we have achieved are reasonably accurate. The other main limitation on the accuracy of our results is the minimum time step we are able to simulate: we would require a higher level of computational power than that which was available to us to run a simulation for a longer amount of time with a time interval much smaller than 10^5s, which means a star may "skip" over an important interaction in its path. We did however manage to run some simulations for much shorter periods of time ($\sim$ 3Myrs) with a time step on the order of 1yr, although this took a long time to process. This limitation caused some erroneous results for some of the TWO family stars, which we handled by reducing the time step as far as possible while still calculating the trajectory for a usable time, and analysing the resulting graphs carefully by eye.

5.3 Note on the Sagittarius Stream

An external source of high velocity objects is the Sagittarius dwarf galaxy (Sag DEG) stream ((Ruhland et al. 2011; Hernitschek et al. 2017)), which produces K and M type giant stars similar to those we have investigated. From literature it has been shown that galactic-stream objects can be identified from their characteristically higher metallicity, with Ren et al. (2017) using the separation $[\frac{Fe}{H}] < -2.0$dex for Galactic Halo stars, however we were unable to introduce this parameter into our project and so we cannot definitively discard the stream as a possible origin. One argument against a Sag DEG stream origin for any of our candidates is found in Ruhland et al. (2011), where the radial velocity distribution for objects in the stream is shown to be largely

within the bound $|v_{rad}| < 250\text{kms}^{-1}$, which is below our lower limit even with errors. This distribution includes data specifically for M type giant stars, sourced from Majewski et al. (2004).

5.4 Future Work

One step we discussed taking but ultimately decided against due to time constraints was performing a spectral analysis of the stars to see if they have any key identifying features such as significant metallicity, which would point to a supernova- or cluster-origin star. Follow up work on this will include adding relativity in the simulations in an attempt to reduce the number of assumptions being made, as well as running simulations for longer time periods at shorter steps on more powerful computers to increase the accuracy of the plots ascertained. Furthermore, while difficult to create, we would also like to simulate the supernova kick, and cluster-origin runaway stars

6 CONCLUSIONS

The results from this work are:

- High velocity stars are rare, and those with the potential to originate from Sagittarius A* are very difficult to find.
- TWO-599 could have been produced by undergoing the Hills mechanism with Sagittarius A*, and although we cannot confirm this reproduced the result using a range of reasonable masses for its hypothetical binary partner, which can be found in stars near Sagittarius A*.
- The rest of our TWO family almost certainly passed close to Sagittarius A*, but likely did not originate in the galactic centre, so the reason for their high velocity is undetermined but nevertheless interesting.
- It is possible that some of our candidate stars originated from the Sagittarius dwarf galaxy stream based on their spectral type, however we cannot prove this.

All the results of our testing, including those which did not produce any identifiable or plausible origin for the stars, have provided us with reasonably confident models of the paths of many high velocity stars, as well as a smaller set of good short-term predictions. Although there are many large sources of error in our data, the fact that we have been able to reproduce directly observable systems to some degree of accuracy in the same simulation through which we ran our candidate stars adds confidence to our results.

ACKNOWLEDGMENTS

We have benefited immensely from the publicly available programming language Python, including NumPy & SciPy (Van Der Walt et al. 2011; Jones et al. 2001), Matplotlib (Hunter 2007), Astropy (Astropy Collaboration et al. 2013) and the Topcat analysis program (Taylor 2013). This research has made use of the VizieR catalogue access tool, CDS, Strasbourg, France. The authors thank *Gaia* for the invaluable data contained in *Gaia* DR2 made accessible in their online archive.

REFERENCES

Abadi M. G., Navarro J. F., Steinmetz M., 2006, MNRAS, 365, 747
Abadi M. G., Navarro J. F., Steinmetz M., 2009, ApJ, 691, L63
Astropy Collaboration et al., 2013, A&A, 558, A33
Blaauw A., 1961, Bull. Astron. Inst. Netherlands, 15, 265
Boubert D., et al., 2019, MNRAS, 486, 2618
Brown W. R., 2015, ARA&A, 53, 15
Capuzzo-Dolcetta R., Fragione G., 2015, MNRAS, 454, 2677
Chatterjee S., Tan J. C., 2012, ApJ, 754, 152
Darbha S., Coughlin E. R., Kasen D., Quataert E., 2019, MNRAS, 482, 2132
Erkal D., Boubert D., Gualandris A., Evans N. W., Antonini F., 2019, MNRAS, 483, 2007
Flynn C., Sommer-Larsen J., Christensen P. R., 1996, MNRAS, 281, 1027
Gillessen S., et al., 2017, The Astrophysical Journal, 837, 30
Greene J. E., Strader J., Ho L. C., 2019, arXiv e-prints, p. arXiv:1911.09678
Gualandris A., Portegies Zwart S., Sipior M. S., 2005, MNRAS, 363, 223
Habibi M., et al., 2017, The Astrophysical Journal, 847, 120
Hattori K., Valluri M., Castro N., Roederer I. U., Mahler G., Khullar G., 2019, ApJ, 873, 116
Hernitschek N., et al., 2017, ApJ, 850, 96
Herrnstein R. M., Zhao J.-H., Bower G. C., Goss W. M., 2004, AJ, 127, 3399
Hills J. G., 1988, Nature, 331, 687
Hoogerwerf R., de Bruijne J. H. J., de Zeeuw P. T., 2001, A&A, 365, 49
Hunter J. D., 2007, Computing In Science & Engineering, 9, 90
Innanen K. A., 1971, in BAAS. p. 441
Irrgang A., Geier S., Heber U., Kupfer T., Fürst F., 2019, A&A, 628, L5
Jones E., Oliphant T., Peterson P., et al., 2001, SciPy: Open source scientific tools for Python, http://www.scipy.org/
Jordan S., 2008, Astronomische Nachrichten, 329, 875
Leonard P. J. T., Duncan M. J., 1990, AJ, 99, 608
Liu C., Bailer-Jones C. A. L., Sordo R., Vallenari A., Borrachero R., Luri X., Sartoretti P., 2012, MNRAS, 426, 2463
Majewski S. R., et al., 2004, AJ, 128, 245
Marchetti T., Contigiani O., Rossi E. M., Albert J. G., Brown A. G. A., Sesana A., 2018, MNRAS, 476, 4697
Poveda A., Ruiz J., Allen C., 1967, Boletin de los Observatorios Tonantzintla y Tacubaya, 4, 86
Rasskazov A., Fragione G., Leigh N. W. C., Tagawa H., Sesana A., Price-Whelan A., Rossi E. M., 2019, The Astrophysical Journal, 878, 17
Ren H.-B., Shi W.-B., Zhang X., Tang Y.-K., Zhang Y., Hou Y.-H., Wang Y.-F., 2017, Research in Astronomy and Astrophysics, 17, 076
Rodriguez C., Taylor G. B., Zavala R. T., Peck A. B., Pollack L. K., Romani R. W., 2006, ApJ, 646, 49
Ruhland C., Bell E. F., Rix H.-W., Xue X.-X., 2011, ApJ, 731, 119
Saroja G., Nuriyah L., 2019, IOP Conference Series: Materials Science and Engineering, 546, 2
Schmidt M., 1956, Bull. Astron. Inst. Netherlands, 13, 15
Schödel R., Merritt D., Eckart A., 2009, A&A, 502, 91
Taylor M., 2013, Starlink User Note, 253
Trenti M., Hut P., 2008, Gravitational N-body Simulations (arXiv:0806.3950)
Van Der Walt S., Colbert S. C., Varoquaux G., 2011, Computing in Science & Engineering, 13, 22
Yu Q., Tremaine S., 2003, ApJ, 599, 1129

APPENDIX A: DATA SELECTION

The selection constraints are given in table A1. Here θ is the parallax angle in milliarcseconds, $\Delta\theta$ is the parallax error, ν_α is the proper motion in milliarcseconds per year ($mas\ yr^{-1}$) in right ascension and similarly ν_δ in declination, v_r is the radial velocity in kms^{-1}, and t_{eff} the effective temperature of the star in Kelvin.

APPENDIX B: DATA FOR ESCAPE VELOCITY

The data used to produce the graph of escape velocity for the Milky Way vs distance from the galactic centre is contained in table B1. The data in the first column is taken from (Flynn et al. 1996), while the second column contains data for a galaxy on the same size scale but with a heavier disk designed to approximate a dark matter halo and produce a range of escape velocities to which to compare our candidate stars.

APPENDIX C: THE TWO FAMILY

For further reference, the full source IDs in the *Gaia* DR2 for 'The TWO Family' of stars are as in table C.

The trajectories of stars TWO-410, TWO-558, and TWO-570 are figures C1, C2, and C3 respectively. Each had a run time of 22 Myr, hence why not all of them show a full trajectory towards Sagittarius A*, however the time step for all was on the order of 100 yr. By comparing the trajectories to that of TWO-558, which does approach Sagittarius A*, it can be determined by inspection that the others are similar enough to regard them as not being of Hills mechanism origin.

This paper has been typeset from a TEX/LATEX file prepared by the author.

Step	Data Set	Constraints	# stars returned	Data used for
Original	*Gaia* DR2	$0.001 < \theta < 1$, $\Delta\theta < 0.2\theta$, $\nu_\alpha \neq 0$, $\nu_\delta \neq 0$, $v_r \neq 0$, $t_{eff} \neq 0$	3,000,000	Further selection
Reduced		$v_{total} > 500$	1158	Simulations
Search TWO	*Gaia* DR2	$\theta < 1$, $\Delta\theta < 0.5\theta$, $\nu_\alpha < 1$, $\nu_\delta < 1$, $v_r > 400$, $\exists t_{eff}$	5	The TWO Family/Simulations

Table A1. The constraints in place for star data selection. Initially we searched for stars from the *Gaia* database that had small parallax, and so their proper motion could not be due to their proximity to Earth; and simply had proper motion and temperature data. This was further reduced to those with a total velocity greater than 500kms^{-1}, as per our definition of a hyper-velocity star. Search TWO was then constrained to give stars with little R.A. and Dec. proper motion, with all their velocities radial.

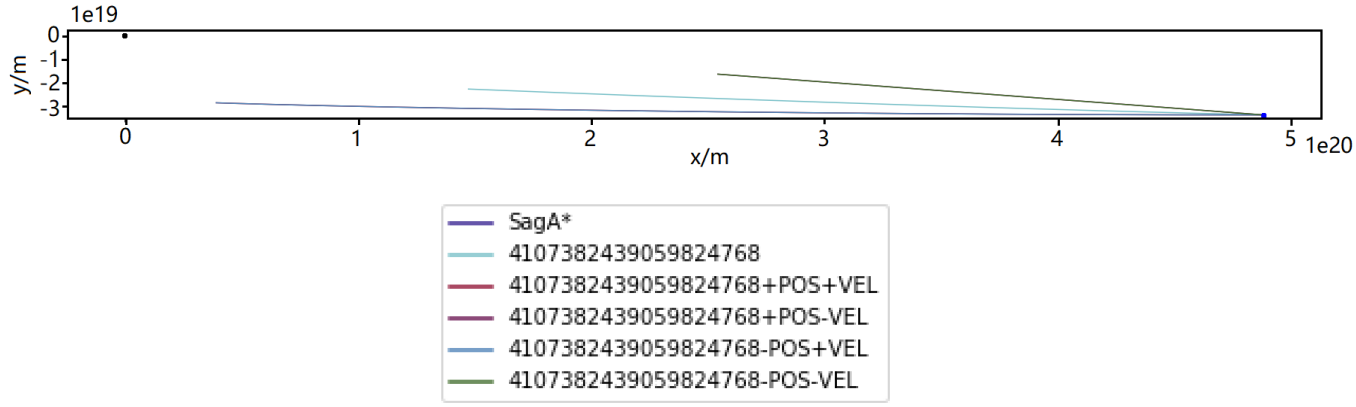

Figure C1. The expected trajectory of TWO-410 in the past 22 Myr. It is seen that the star had an origin near to Sagittarius A*, but extrapolating the trajectory reveals that it does not pass close enough to the black hole to be considered of having its true origin there.

Component	**Original Values**	**Heavy Version**
R_{C1}	$0.42kpc$	$0.42kpc$
M_{C1}	$3.0 \times 10^9 M_\odot$	$3.0 \times 10^9 M_\odot$
R_{C2}	$2.7kpc$	$2.7kpc$
M_{C2}	$1.6 \times 10^{10} M_\odot$	$1.6 \times 10^{10} M_\odot$
a_1	$5.81kpc$	$5.81kpc$
a_2	$17.43kpc$	$17.43kpc$
a_3	$34.86kpc$	$34.86kpc$
M_{D1}	$6.6 \times 10^{10} M_\odot$	$13.2 \times 10^{10} M_\odot$
M_{D2}	$-2.9 \times 10^{10} M_\odot$	$-5.8 \times 10^{10} M_\odot$
M_{D3}	$3.3 \times 10^9 M_\odot$	$6.6 \times 10^9 M_\odot$
b	$0.306kpc$	$0.306kpc$
z	0	0

Table B1. Table of values used in the galactic potential models.

Star Name	*Gaia* Source ID
TWO	4662254521025223680
TWO-410	4107382439059824768
TWO-558	5588591555569392512
TWO-570	5709258382570534272
TWO-599	5990629356697925120

Table C1. The source IDs of the TWO Family of stars.

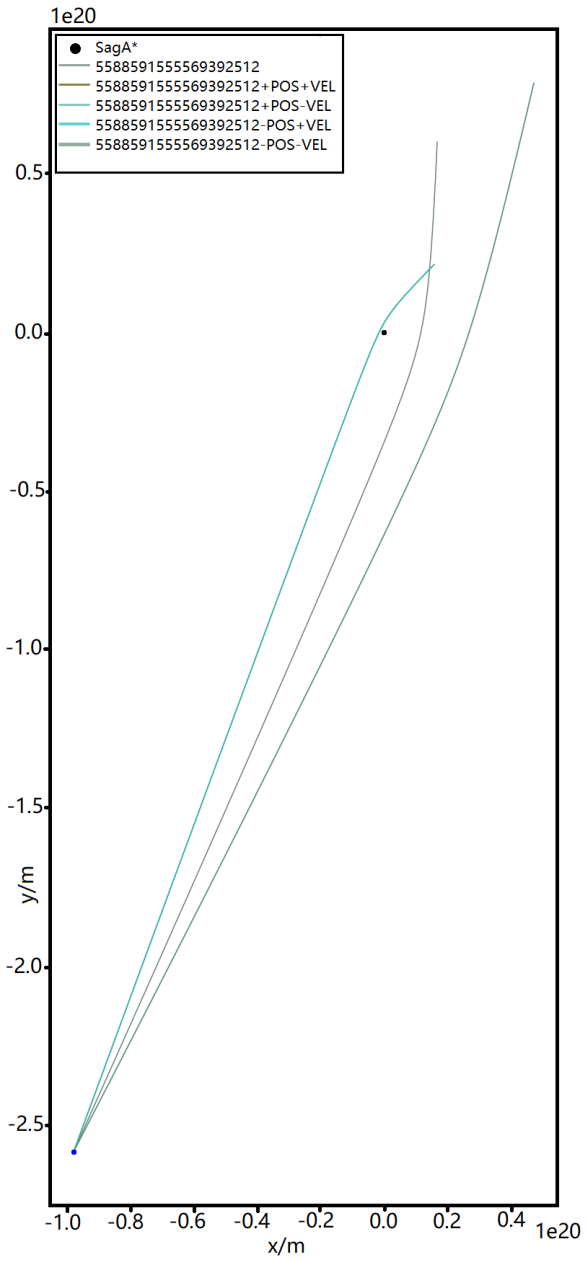

Figure C2. The expected trajectory of TWO-558 in the past 22 Myr. TWO-588 clearly interacts with Sagittarius A*, and within error could have passed close enough to be considered as being of Hills Mechanism origin, but due to the large error this was discounted as such.

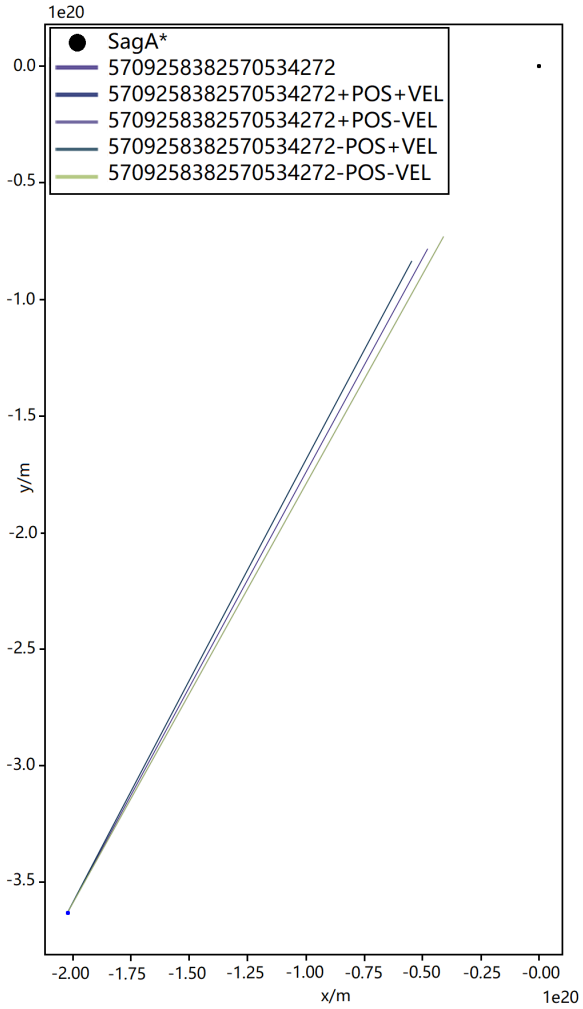

Figure C3. The expected trajectory of TWO-570 in the past 22 Myr. The star is seen to approach Sagittarius A* in its past, but would not be close enough to be considered of Hills Mechanism origin.